



Design and synthesis of $Zn_{0.3}Fe_{0.45}O_3$ nanoparticle for efficient removal of Congo red dye and its kinetic and isotherm investigation

Ganesh Jethave¹ · Umesh Fegade¹

Received: 31 August 2017 / Accepted: 9 March 2018 / Published online: 27 March 2018
© The Author(s) 2018

Abstract

$Zn_{0.3}Fe_{0.45}O_3$ bimetallic oxide nanoparticle (ZnFeBONp) was synthesized and characterized by FESEM, EDS, XRD, BET, TEM and FT-IR techniques with the aim of exploring its application for removing of Congo red dye from waste samples. The effects of pH, contact time, adsorbent dosage and dye concentration on the removal of dye were investigated and optimized as pH 6.5, 40 min contact time, 0.2 g adsorbent dose for 20 ppm dye. Results indicated that the synthesized adsorbent could effectively remove high concentrations of dye in a short contact time. Isotherm modeling revealed that the Langmuir isotherm could better describe the adsorption of the dye on the ZnFeBONp as compared to other models. The q_{max} up to 333.33 mg g⁻¹. The results showed that the adsorption system followed the Ho and McKay equations for the entire adsorption. Kinetics of Congo red adsorption on ZnFeBONp best fit with the pseudo-second-order model. Because of the high-specific surface area and nano-scale particle size, ZnFeBONp indicated favorable adsorption behavior for dye.

Keywords ZnFeBONp · Isotherm modeling · Ho and McKay equations · Pseudo-second-order model

Abbreviations

α_L	Langmuir isotherm constant (L mg ⁻¹)
C_0	Initial dye concentration in liquid phase (mg L ⁻¹)
C_e	Liquid phase dye concentration at equilibrium (mg L ⁻¹)
K_s	Equilibrium rate constant of pseudo-second-order adsorption (g mg ⁻¹ min ⁻¹)
K_f	Freundlich constant (L g ⁻¹)
K_L	Langmuir isotherm constant (L g ⁻¹)
q_e	Amount of dye adsorbed at equilibrium (mg g ⁻¹)
q_t	Amount of dye adsorbed at time t (mg g ⁻¹)
Q_{max}	Maximum adsorption capacity of the adsorbent (mg g ⁻¹)
m	Mass of adsorbent used (g)
n	Freundlich isotherm exponent
R^2	Linear correlation coefficient

V	Volume of dye solution (L)
R_L	Separation factor

Introduction

Water pollution due to industrial dye effluent is a very serious problem which undergoes chemical as well as biological changes, consume dissolved oxygen, and destroy aquatic life [1–3]. Dyes are used in various industries such as construction, textile, paper, plastics, leather, cosmetics, etc., for the purpose of coloring the related products. Therefore, large amount of colored wastewater is produced. Many dyes are highly poisonous, carcinogenic, and stable from daylight and oxidation. Dyes not only make water colorful but also do harm for the survival of aquatic life and the ecosystem [2]. For example, dyes will deadly affect the photosynthetic aquatic life due to the reduction of light penetration [3]. Thus, the researcher working for developing an effective and suitable way to eliminate dye contamination from wastewater has become an urgent issue.

Till date, several techniques, such as coagulation, biological treatment, chemical oxidation, photocatalytic degradation and adsorption, have been explored to remove the dye contaminants from wastewater [4–7]. Adsorption is a more competitive method for removal of dyes due to

Electronic supplementary material The online version of this article (<https://doi.org/10.1007/s40090-018-0140-9>) contains supplementary material, which is available to authorized users.

✉ Umesh Fegade
umeshfegade@gmail.com

¹ Department of Chemistry, Bhusawal Arts, Science and P. O. Nahata Commerce College, Bhusawal, MH, India

its high efficiency and economy. Currently, adsorption has been proved to be a simple and time-saving technology for removal of dyes [8], in which the key technology is to exploit selective and efficient adsorbents [9, 10]. Conventional adsorbents such as silica gel [11], activated alumina [12] and zeolite molecular sieve [13, 14], displayed low removal efficiency.

In last few years, we synthesized the organic receptor for the selective and sensitive detection of metal ion and removal of phosphate from waste water [15–23]. In the current study, we report the synthesis of ZnFeBONP and explore its ability to remove Congo red (CR) from aqueous solution. Congo red was taken as models for azo dyes, for removal investigation. For the present study, a batch-contact-time method was used, and the equilibrium of CR adsorption on to ZnFeBONP was investigated with attempts to fit the data to Langmuir, Freundlich and Temkin equations. The uptake of CR on ZnFeBONP was examined as a function of adsorbate concentration, adsorbent concentration and contact time. The kinetic order and thermodynamic parameter was deduced on CR adsorption on ZnFeBONP (Scheme 1).

Materials and method

Instrumentation

A Metrohm model 713 pH-meter was used for pH measurements. Field emission scanning electron microscopy (FE-SEM) images were obtained with a Bruker S-4800 instrument operated at 15.0 kV. EDX was done on the same instrument at PM Image size: 500×375 Mag:40,000 \times HV:15.0 kV. X-ray diffraction (XRD) pattern was recorded by X-ray diffractometer (Germany, Bruker D8-advance, Cu K α $k = 1.54056$ nm) for 2θ values over 10 – 70° . The UV–Vis spectra were recorded on

Shimadzu UV-1800 spectrophotometer at room temperature using quartz cell of 1 cm path length, multipoint Brunauer–Emmery–Teller (BET) method were used for the determination of specific surface area of the nanoparticle from the N₂ adsorption data at the relative pressure (P/P_0) range of 0.05–1.0, FT-IR spectrum has been taken using Bruker instrument and in the range of 4000 – 500 cm⁻¹.

Reagents and materials

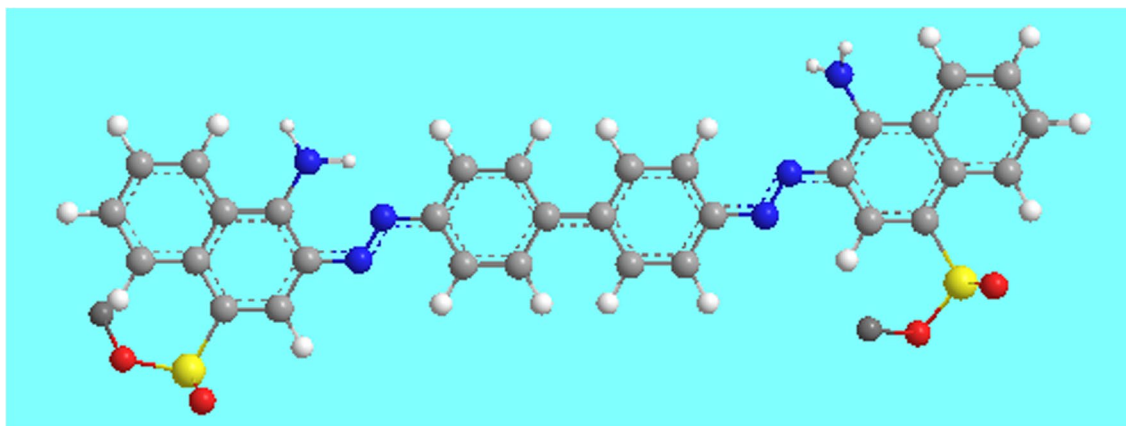
All the chemicals and reagents used in this work were of analytical grade and purchased from Merck (Merck, Darmstadt, Germany). The water used for aqueous phase was MiliQ water (A Grade) in every stage of the study.

Synthesis of ZnFeBONP

The ZnFeBONP were synthesized according to a co-precipitation method followed by magnetic stirring. First, 4.5 g of ZnCl₂ and 7.4 g of FeCl₃ were added to 300 ml of DW. Then, 35 ml of 1 M NaOH solution was added to the former solution dropwise. The whole solution is then stirred with magnetic stirrer for 2 h at 60 °C temperature, leading to smaller and more homogenized particles. A brown precipitate quickly formed, which was allowed to crystallize completely for another 30 min. The precipitate was washed with DW by magnetic decantation until the pH of the suspension was less than 7.5. The suspension was filtered by means of suction pump, after filtration precipitate was dried at about 100 °C and then crush into powder and use for further study.

Solution preparation and adsorption behavior

Adsorption behavior was performed by adding 0.05 g of ZnFeBONP to the 50 ml of CR solution in a 100 ml conical flask. The pH of the CR solution was adjusted



Scheme 1 Molecular structure of Congo red (CR)

at 6.5 using 0.01 mol L^{-1} HCl or 0.1 mol L^{-1} NaOH and the solution was shaken on rotary shaker at 200 rpm for 90 min. The aliquot taken from the solution at a fixed time point was centrifuged at 2000 rpm for 3 min. The concentration of CR in the solution was measured spectrophotometrically at 498 nm. The concentration of CR decreased with time due to its adsorption by ZnFeBONP.

The adsorption capacity of each dye in the adsorption system, q_e , was calculated by

$$q_e = (C_i - C_e)V/m, \quad (1)$$

where C_i and C_e are initial and equilibrium concentrations

much smaller than the SEM morphology shown in Fig. 1a and it is good in terms of adsorption point of view. EDX was used to observe the elemental composition of the samples. The results reveal that the sample is composed of Zn, Fe and O in which the concentrations are about 21.76, 26.94 and 51.29 wt%, respectively (Fig. 1b). A FT-IR spectrum of ZnFeBONP is presented in Fig. 2. The absorption bands below 687 cm^{-1} is attributed to Fe–O stretching vibrational modes. The peak at 1631 cm^{-1} is ascribed to the O–H bending vibration of adsorbed water molecules and the broad absorption band at 3372 cm^{-1} corresponds to the O–H stretching region. The observed peak at 1351 cm^{-1} in the

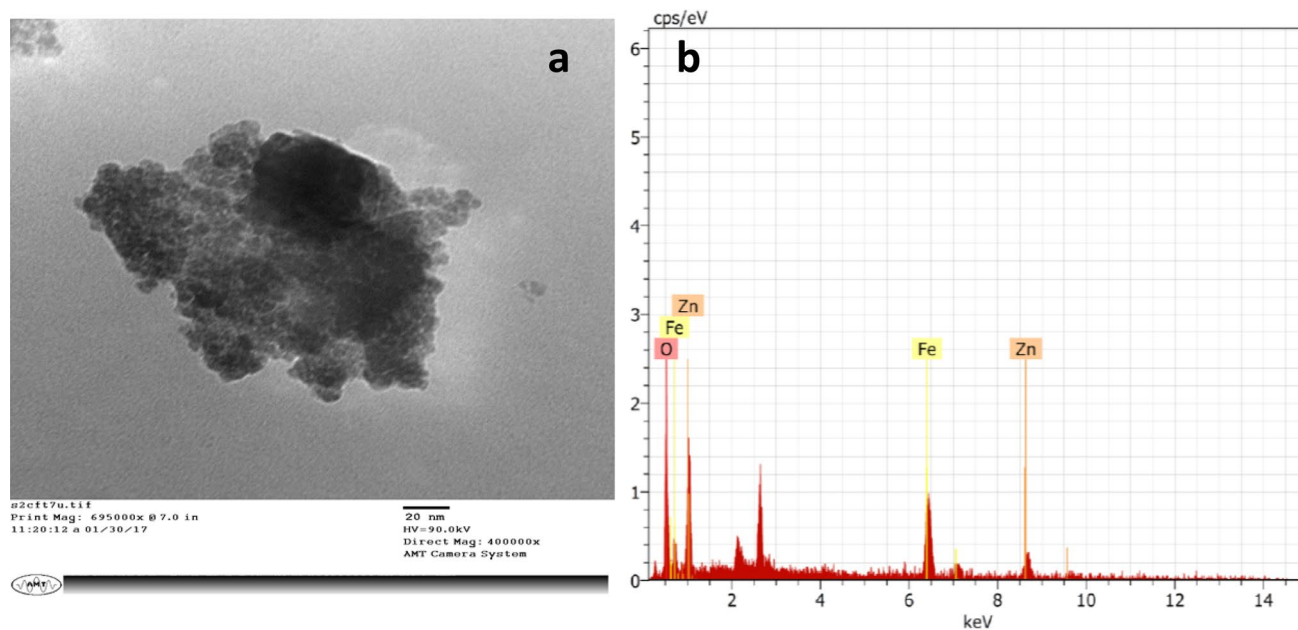


Fig. 1 a TEM image of NPs. b EDX spectra of the ZnFeBONP

(mg L^{-1}), respectively, m is the mass of the adsorbent (g); and V is volume of the solution (L).

Results and discussion

Characterization

The ZnFeBONP were synthesized according to a co-precipitation method at constant temp $60 \text{ }^\circ\text{C}$ with stirring. Figure S1a (Supplement file) shows typical SEM images of the ZnFeBONP. As shown in Fig. S1a, it is found that the product is composed of a large quantity of nanostructures. The low magnification image shows the particle size and the average size of nanoparticle was 37.72 nm . The TEM image of ZnFeBONP nanoparticles was shown in Fig. 1a, and the average particle size was about 20 nm , which is

FT-IR spectrum of ZnFeBONP may be endorsed to C–O single bond. The band appeared at 1473 cm^{-1} may be due to C–H bending vibration. In Fig. 3, it could be seen that the curve belonged to the nitrogen sorption isotherm whose adsorption curve was not coincident with desorption curve thus forming a hysteresis loop. The calculated specific surface area was $133.3 \text{ m}^2 \text{ g}^{-1}$. The X-ray diffraction patterns of ZnFeBONPs are shown in Fig. 4. Significant X-ray diffraction peaks occurred at 31.24° , 34.35° , 36.29° , 56.19° , 62.63° and 67.80° corresponds to reflection from (1 1 1), (2 0 0), (0 0 2), (1 0 2), (3 1 1) and (2 0 0) miller planes of ZnFeBONPs and the corresponding peaks became stronger and narrower, which implied that the crystallinity was higher. The structural characterization results obtained from the XRD pattern reveals that the powder is polycrystalline (cubic and hexagonal lattice).



Effect of pH solution

pH of solution has very deep impact on the adsorption process. In this study, the adsorption experiments have been conducted in the initial pH range from 5.0 to 8.5 and the corresponding result is shown in Fig. 5. The effect of the solution pH on the adsorption of dye onto ZnFeBONP was assessed at different values, ranging from 5 to 8.5. In these experiments, the initial concentration of dye and adsorbent dosage were set at 20 mg L^{-1} and 0.05 g , respectively, for all batch tests in this experiment. The % adsorption is maximum at pH 6.5 that is 98.88%. Therefore, further parameters were performed at pH 6.5. The surface of metal oxides is generally covered with hydroxyl groups that vary in form with pH. The experimentally calculated pH_{zpc} of ZnFeBONPs is 7.1. The surface charge is positive at pH values lower than pH_{zpc} , neutral at pH_{zpc} , and negative at pH values higher than it. Therefore, adsorption efficiency decreases at pH value higher than 6.5.

Effect of time variation

The effect of contact time is a very crucial factor which persuades the adsorption of dye pollutant from wastewater. For this purpose, 50 mL of desired (20 mg L^{-1} CR dye) solution was prepared and further it was treated with 50 mg of adsorbent at 298 K, the CR were separated from aqueous solutions and the residual concentration of dye pollutant in aliquot were measured by spectrophotometric method. The results show a very high adsorption rate at initial times which is recognized to the high concentration of adsorption sites on the surface and strong interaction between the adsorbate and adsorbent (Fig. 6). Over time, the concentration gradient reduces due to the adsorption of CR molecules onto the adsorbent and leads to a lower adsorption during the later stages. The graph shows that within 20 min the 88% dye was adsorbed and at 40 min the adsorption reaches up to 92% and remains constant.

The effect of adsorbent concentration

The effect of ZnFeBONP quantity for % adsorption was investigated by adding various amounts of adsorbent in

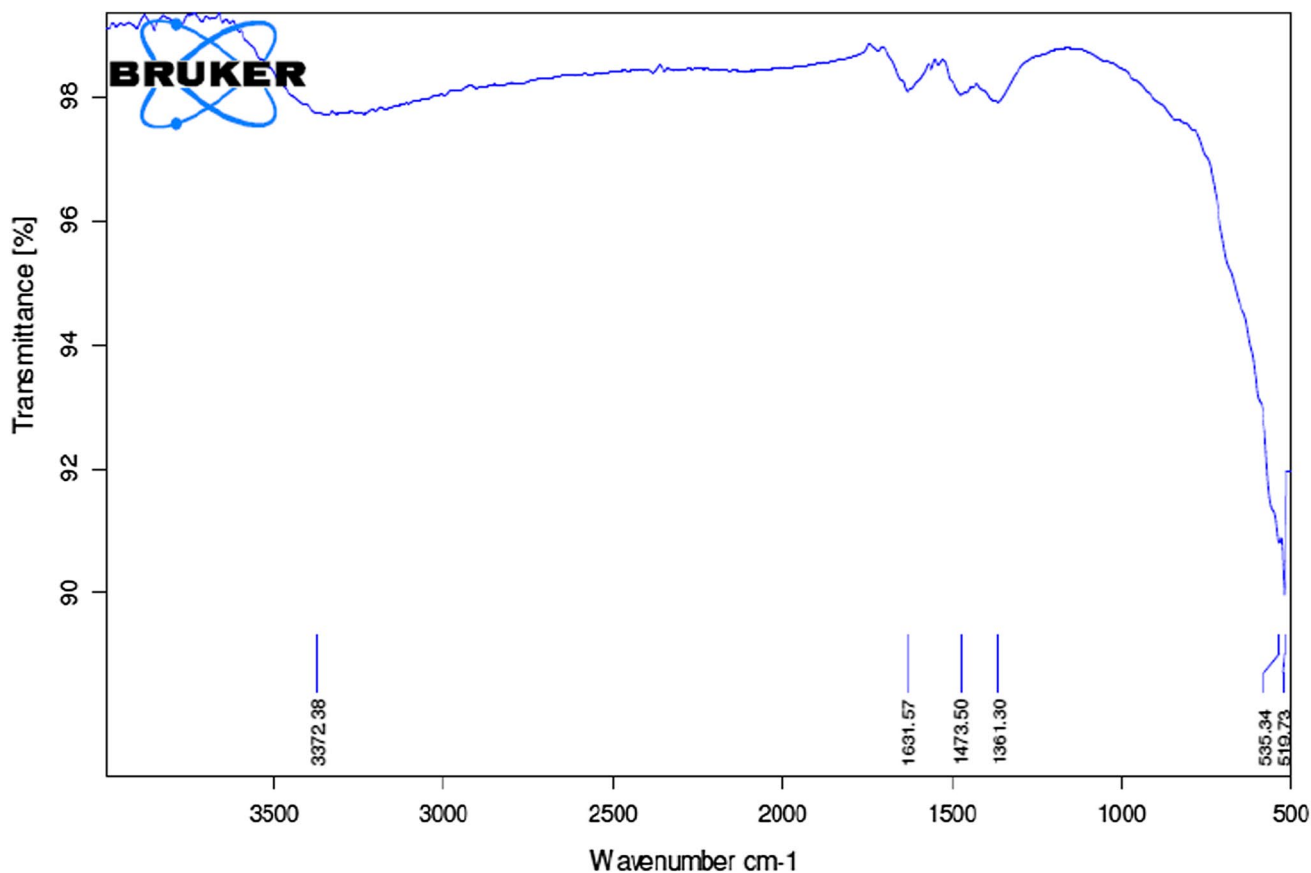


Fig. 2 IR spectrum of the ZnFeBONP



Fig. 3 N_2 sorption isotherm of magnetic ZnFeBONPs calcined at 450 °C for 1.5 h with absolute alcohol of 20 mL

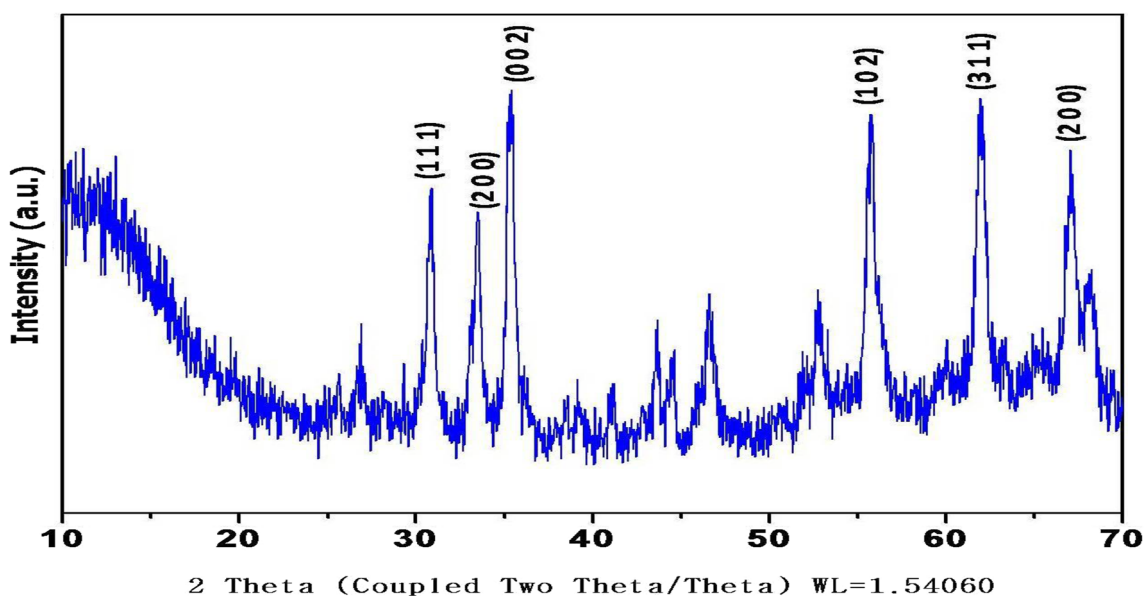
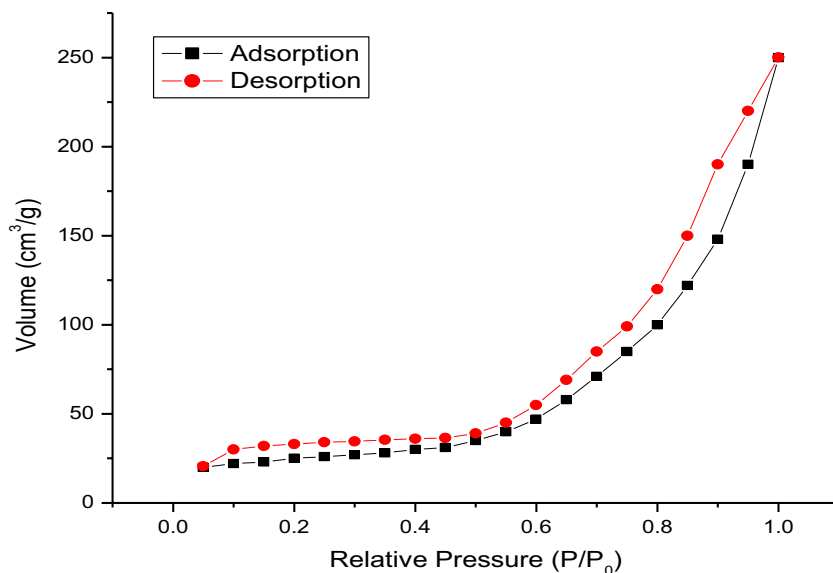


Fig. 4 XRD patterns of ZnFeBONPs

the range 0.05–0.2 g into the beaker containing 50 mL of dye solution (20 mg L^{-1}) at pH 6.5 and 25 °C for all batch experiments. The results are shown in Fig. 7 and indicated that addition of 0.2 g of adsorbent per 50 mL solution of dye (20 mg L^{-1}) lead to maximum adsorption of dye. The supernatant was analyzed for the remaining dye. The results showed that the adsorption efficiencies increased by increasing adsorbent dose. It was observed that by increasing the ZnFeBONP dosage from 0.05 to 0.2 g, the removal efficiency (%) of dye increased from 69.51 to 92.88%. This observation can be explained by

the greater number of adsorption sites made available at greater ZnFeBONP dosages. Above 0.2 g of ZnFeBONP dosage, the adsorption equilibrium of dye was reached and the removal ratio of dye held almost no variety. Nevertheless, the adsorption capacity initially increased and then decreased as the ZnFeBONP dosage increased.

Chemical kinetic models (pseudo-second-order)

The pseudo-second-order model, proposed by Ho and McKay, can be represented in the following linear form [23].

Fig. 5 Effect of initial pH of dye solution on removal of CR (ZnFeBONP dosage=0.05 g, initial dye concentration=20 mg L⁻¹, stirring time=90 min)

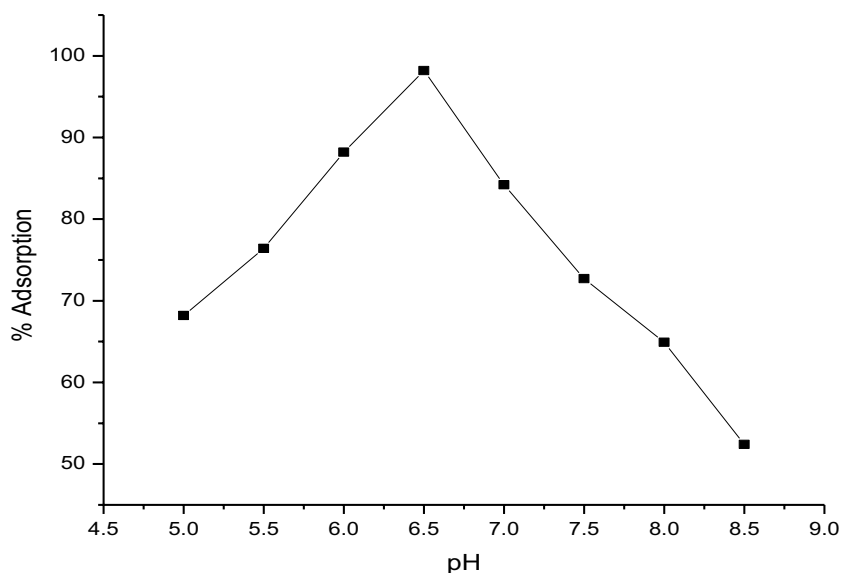
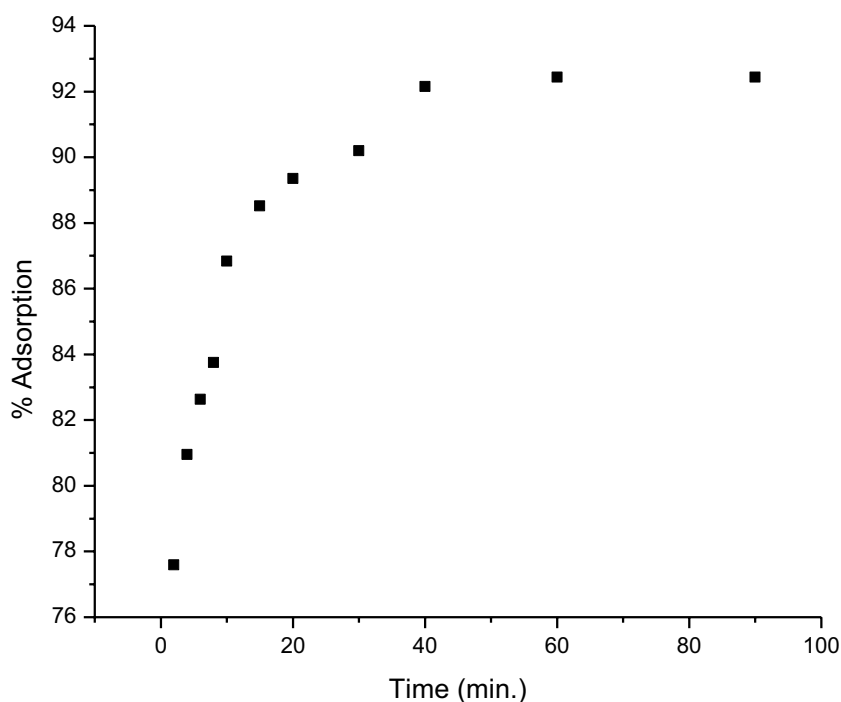


Fig. 6 Effect of contact time on the adsorption of CR on the ZnFeBONP surface



In this model, plotting the t/q_t of experimental data versus t is used to show its suitability for explanation of whole adsorption data. It was found that the plot of t/q_t versus t is a straight line. The high and reasonable values of R^2 and closeness of experimental and theoretical (q_e) value indicate this model ability for explanation of adsorption process over the whole concentration range. Sorption kinetic studies were conducted at RT under initial dye concentration of 20 mg L⁻¹. Adsorption kinetics were studied using kinetic model, namely the pseudo-second-order model.

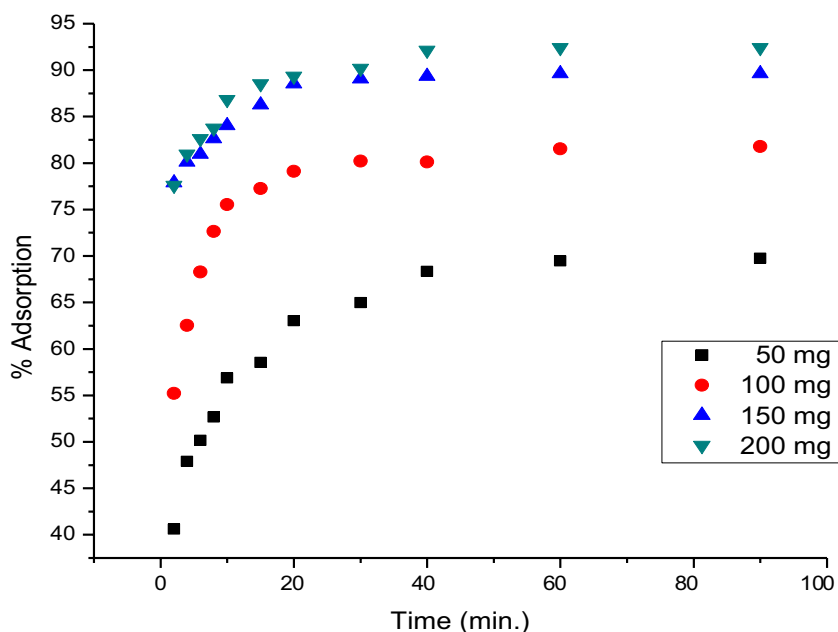
The pseudo-second-order kinetic model is described by the formula

$$t/q_t = 1/k_{ad}q_e^2 + t/q_e \quad (2)$$

The results showed that the adsorption system followed the Ho and McKay equations for the entire adsorption. Kinetics of Congo red adsorption on ZnFeBONP best fit the pseudo-second-order model, suggesting that the adsorption mechanism depends on the adsorbate and adsorbent, and the rate-limiting step may be chemisorption involving valence forces through the sharing or



Fig. 7 Effect of adsorption of CR to ZnFeBONP at different initial ZnFeBONP concentrations (at 25 °C, pH 6.5)



exchange of electrons. This confirmed that adsorption of dye takes place probably via surface exchange reactions until the surface functional sites are fully occupied.

Adsorption isotherms

The equilibrium adsorption isotherm model, which is the number of mg adsorbed per gram of adsorbent (q_e) vs. the equilibrium concentration of adsorbate (Fig. 9a), is fundamental in describing the interactive behavior between adsorbate and adsorbent. Analysis of isotherm data is important for predicting the adsorption capacity of the adsorbent, which is one of the main parameter required for the design of an adsorption system. Equilibrium isotherm studies were carried out with different initial concentrations of CR (50–200 mg L⁻¹) at 25 °C and pH 6.0. Three models were used to analyze the equilibrium adsorption data: Langmuir, Freundlich and Temkin [24, 25]. Langmuir's model does not take into account the variation in adsorption energy, but it is the simplest description of the adsorption process. It is based on the physical hypothesis that the maximum adsorption capacity consists of a monolayer adsorption, that there are no interactions between adsorbed molecules, and that the adsorption energy is distributed homogeneously over the entire coverage surface.

The general form of the Langmuir isotherm is:

$$q_e \alpha_L / K_L = K_L C_e / (1 + K_L C_e), \quad (3)$$

where C_e is the equilibrium concentration of the CR in the solution (mg L⁻¹), q_e is the amount of CR adsorbed per unit

mass of adsorbent (mg g⁻¹), at equilibrium concentration, C_e , α_L (L mg⁻¹) and K_L (L g⁻¹) are the Langmuir constants with α_L related to the adsorption energy and q_{max} [= K_L/α_L] signifies the maximum adsorption capacity (mg g⁻¹), which depends on the number of adsorption sites. The Langmuir isotherm shows that the amount of anions adsorbed increases as the concentration increases up to a saturation point. As long as there are available sites, adsorption will increase with increasing CR concentrations, but as soon as all of the sites are occupied, a further increase in concentrations of CR solutions does not increase the amount of CR on adsorbents (Table 1).

After linearization of the Langmuir isotherm, Eq. (3), we obtain

$$C_e/q_e = C_e \alpha_L / K_L + 1/K_L. \quad (4)$$

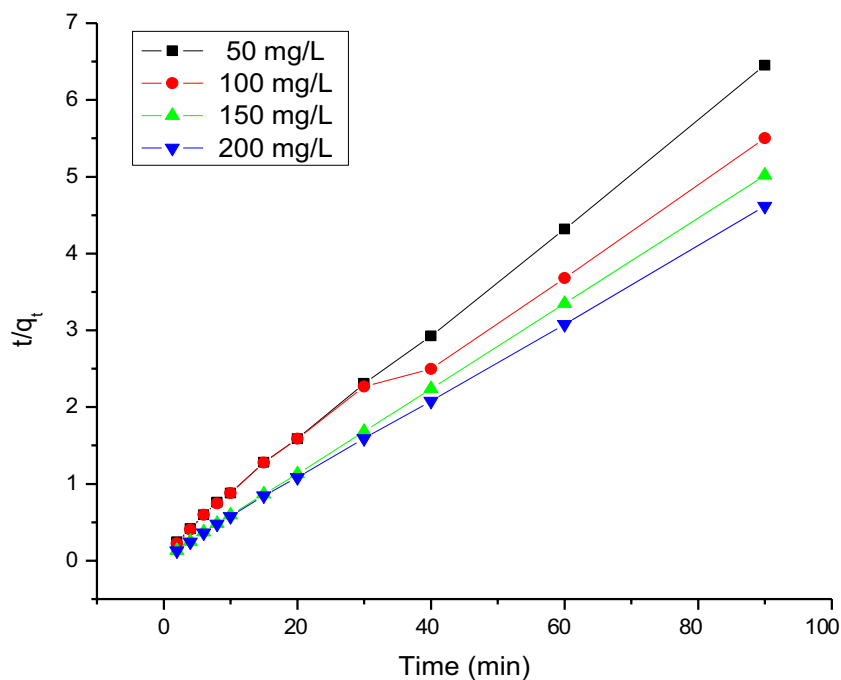
The values of α_L and K_L are calculated from the slope and intercept of the plot of C_e/q_e vs. C_e (Fig. 8). The amount of CR adsorbed (mg g⁻¹) was calculated based on a mass balance equation as given below:

$$q_e = V(C_o - C_e)/m, \quad (5)$$

where C_o is the initial concentration of CR in mg L⁻¹, V is the volume of experimental solution in L, and m is the dry weight of nanoparticles in g. The parameters of the Langmuir equation were calculated and are given in Table 2. Table 2 indicates that the maximum adsorption capacity of ZnFeBONP ($q_{max} = 333.33$ mg g⁻¹) for CR is very much higher than that of other adsorbents.

Table 1 Percentage composition of metal present in the sample

El	AN	Series	Unn. C (wt%)	Norm. C (wt%)	Atom. C (at%)	Error (1 Sigma) (wt%)
O	8	K-series	13.69	21.89	51.29	3.42
Fe	26	K-series	25.10	40.14	26.94	1.23
Zn	30	K-series	23.75	37.97	21.76	1.85
		Total	62.54	100.00	100.00	

Fig. 8 Pseudo-second-order adsorption kinetic plots of CR onto ZnFeBONP at different initial dye concentrations

The Freundlich equilibrium isotherm equation was also used to describe experimental adsorption data. This isotherm is an empirical equation which is used for the description of multilayer adsorption with interaction between adsorbed molecules. The Freundlich isotherm is the earliest known relationship describing the adsorption equation. The Freundlich empirical model is represented by

$$q_e = K_f C_e^{1/n}, \quad (6)$$

where C_e is the equilibrium concentration (mg L^{-1}), q_e is the amount adsorbed at equilibrium (mg g^{-1}), and K_f (mg g^{-1}) and $1/n$ are Freundlich constants depending on the temperature and the given adsorbent–adsorbate couple. n is related to the adsorption energy distribution, and K_f indicates the adsorption capacity. The linearized form of the Freundlich adsorption isotherm equation is

$$\ln q_e = \ln K_f + \ln C_e/n. \quad (7)$$

The values of K_f and $1/n$ calculated from the intercept and slope of the plot of $\ln q_e$ vs. $\ln C_e$ (Fig. 9b) are listed in Table 2. Table 2 shows that the values of correlation

Table 2 Data deduced from Langmuir, Freundlich and Temkin isotherm plot

Langmuir isotherm		Freundlich isotherm		Temkin isotherm	
$1/K_L$	0.262	$\ln K_f$	4.098	B	0.029
$q_{\max} = K_L/\alpha_L$	333.33	$1/nf$	0.399	$B \ln KT$	1.441
R^2	0.993	R^2	0.979	R^2	0.975

coefficient R^2 for the fit of experimental isotherm data to Langmuir equation is more close to 0.964 than that of Freundlich equation. Therefore, the Langmuir model represents the experimental data better on the basis of values of regression coefficients.

The Temkin isotherm contains a factor that explicitly accounts the interaction between adsorbing species–adsorbent. The Temkin equilibrium isotherm equation was also used to describe experimental adsorption data (Fig. 9c). The heat of the adsorption and the adsorbent–adsorbate interaction using Temkin isotherm model were evaluated [26].

$$q_e = B_1 \ln KT + B_1 \ln C_e, \quad (8)$$

where C_e is the equilibrium concentration (mg L^{-1}), q_e is the amount adsorbed at equilibrium (mg g^{-1}), B is the Temkin constant related to heat of the adsorption (J mol^{-1}), T is the absolute temperature (K), R is the universal gas constant ($8.314 \text{ J mol}^{-1} \text{ K}^{-1}$), KT is the equilibrium binding constant (L mg^{-1}). The values of the Temkin constants and the correlation coefficient are lower than the Langmuir value. Therefore, the Langmuir isotherm provides the best correlation for the experimental data. The correlation coefficients R^2 obtained from Temkin model were comparable to that obtained for Langmuir and Freundlich equations, which explain the applicability of Temkin model to the adsorption of CR onto ZnFeBONP.

Separation factor

The essential feature of the Langmuir isotherm can be expressed in terms of a dimensionless constant separation factor (R_L) given by the following equation:

$$R_L = 1/(1 + \alpha_L C_0), \quad (9)$$

R_L values within the range $0 < R_L < 1$ indicate favorable adsorption (Fig. 9d) [27]. In this study, R_L value of ZnFe-BONP for the initial CR concentration of 50 mg L^{-1} , obtained as 0.0476, indicate favorable adsorption of CR onto them. The Freundlich isotherm model is an empirical equation that describes the surface heterogeneity of the sorbent. It considers multilayer adsorption with a heterogeneous energetic distribution of active sites, accompanied by interactions between adsorbed molecules.

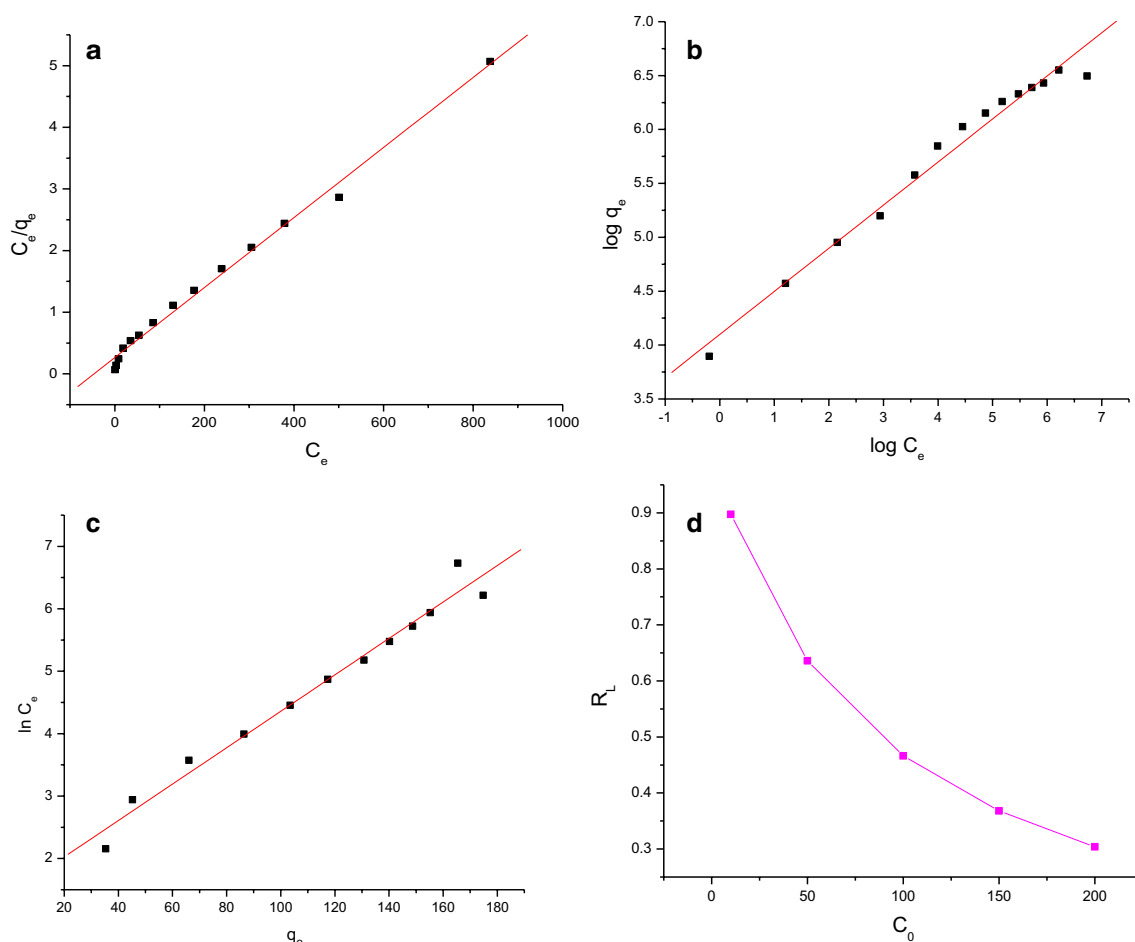


Fig. 9 a Linearization of the Langmuir isotherm. b Freundlich isotherm plot. c Temkin isotherm plot. d Separation factor

Adsorption thermodynamic parameters

Thermodynamic parameter related to the adsorption process i.e., free energy change (ΔG , kJ mol^{-1}) for adsorption at $25\text{ }^\circ\text{C}$ was calculated using the following equation:

$$\Delta G = -RT \ln K_L, \quad (10)$$

where R is the universal gas constant ($8.314\text{ J mol}^{-1}\text{ K}^{-1}$), T is the temperature and K_L is Langmuir constant (L mol^{-1}) obtained from the plot of C_e/q_e versus C_e . The calculated ΔG value was found to be $-2.430\text{ kJ mol}^{-1}$. The negative value of free energy change indicated the spontaneous nature of sorption and confirmed affinity of adsorbent for the dye [28, 29].

Regeneration of ZnFeBONP by heating

Regeneration capacity of an adsorbent shows the cost effectiveness of the adsorbent and this over-all process plays a key role in its commercial application. The regeneration was conducted by calcinations of used ZnFeBONP at $300\text{ }^\circ\text{C}$ for 2 h. During calcinations, the adsorbed organic components were driven-off by its oxidative decomposition along with desorption of water molecules. Adsorption studies over regenerated ZnFeBONP were carried out at pre-optimized conditions. The process of regeneration and recycle of the adsorbent was carried out three times to confirm the performance in CR removal. The adsorption capacity after successive regeneration and use is presented in Fig. 10. After first regeneration, the ZnFeBONP exhibited about 5% lower adsorption capacities than the fresh sample. However, after second and third regenerations, the adsorption capacity remained constant. This suggests that, ZnFeBONP can

be regenerated by calcination process with an acceptable adsorption capacity.

Industrial applications

The most important feature of any research is that it can be suitably applied for industry and environment. In the current work, synthesized ZnFeBONP adsorbent is applied to dye removal of industrial waste samples. The variation in removal percentage, particularly at higher sample volume and concentration of dye molecule must not exceed $\pm 5\%$ to suppose that the method can be applied as pilot plant. The efficiency of the present adsorbents for the removal of CR from real effluents was examined using two effluent streams. Thereafter, in our experiments, 50 mL of concentrated wastewater was diluted to 500 mL, and optimized procedure was carried out. The result shows the significant adsorption of CR take place, when the volume is large but again we carried out experiment at high volume and concentration. In all the examined approaches, using 0.2 g of adsorbent for 1 h, more than 98% of CR removal was achieved. All the experimental conditions, results and comparison data with other material are shown in [30–42] Tables 3 and 4, respectively. It was found that in most cases, more than 98% of dye removal was achieved. This confirms the usefulness of the adsorbent for the CR dye removal.

Fig. 10 Influence of regeneration of ZnFeBONP by calcinations on adsorption capacity

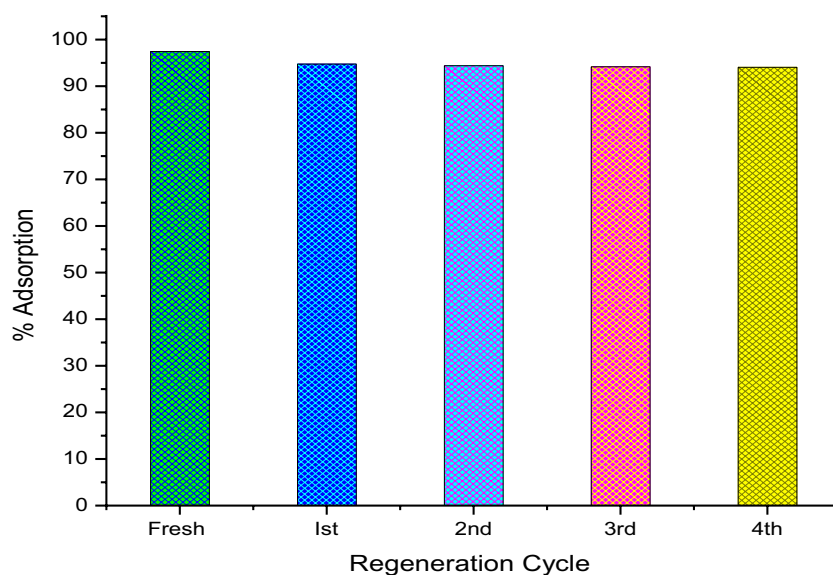


Table 3 Direct application of Pb-FeONPs on waste of laboratory and industrial waste samples

Sample	Sample no.	Initial dye concentration (mg L ⁻¹)	Removal (%)	Average	RSD
Waste of laboratory	1	50	98.12	97.97	0.15
	2		97.82		
	3		97.98		
Industrial waste sample	1		98.12	98.46	0.37
	2		98.86		
	3		98.42		

Table 4 Comparison of maximum adsorption capacities of different adsorbents with ZnFeBONP

Adsorbents	Q max value (mg g ⁻¹)	References
NiO–SiO ₂ composite	204.10	Chunsheng Lei et al. (2015)
Magnetic Ni _{0.5} Zn _{0.5} Fe ₂ O ₄	204.82	Ruijiang Liu et al. (2015)
Magnetic CoFe ₂ O ₄ nanoparticles	93.74	Ruijiang Liu et al. (2016)
Mesoporous ZrO ₂ fibers	103.46	Zhichao Yu et al. (2016)
CoFe ₂ O ₄ nanoparticles	241.50	Xiaofei Wu et al. (2016)
Porous zinc oxide (ZnO) microspheres	334.00	Chunsheng Lei et al. (2016)
Ni(OH) ₂	384.60	Yingqiu Zheng et al. (2017)
NiO	534.80	Yingqiu Zheng et al. (2017)
PPy/m _w nanocomposite	147.00	R. S. Aliabadi et al. (2018)
Aluminum-based nanosheet (AlNs)	121.95	Anu Mary Ealias et al. (2018)
Flower-like MgO-GO microspheres	237.00	Jing Xu et al. (2018)
Flower-like MgO microspheres	228.00	Jing Xu et al. (2018)
ZnFeBONPs	333.33	Present study

Conclusion

ZnFeBONP were synthesized according to a co-precipitation method at constant temp 60 °C with stirring an average size distribution of 37.72 nm and utilized it as an efficient adsorbent for removing of Congo red from wastewater samples. The effects of pH, contact time, adsorbent dosage, dye concentration on the removal of dye were investigated separately through batch experiments. Results indicated optimized pH 6.5, 40 min contact time, 0.2 mg adsorbent dose for 20 ppm dye. Isotherm modeling revealed that the Langmuir isotherm could better describe the adsorption of the dye onto the ZnFeBONP as compared to other models. Because of the high-specific surface area and nano-scale particle size, ZnFeBONP indicated favorable adsorption behavior for dye. The results showed that the adsorption system followed the Ho and McKay equations for the entire adsorption. Kinetics of Congo red adsorption on ZnFeBONP best fit the pseudo-second-order model. At the end of this study, we can say that the modified ZnFeBONP nanoparticles may be used as an alternative sorbent for the removal of some dye molecules from wastewaters.

Acknowledgement The authors are thankful to the Principal Prof. Dr. M. V. Waykole, President of TES Management Dr. M. M Phalak and Chairman of TES Management M. D. Phalak of the Bhusawal Arts,

Science and P. O. Nahata Commerce College, Bhusawal, (MH), India, for providing necessary laboratory facilities.

Open Access This article is distributed under the terms of the Creative Commons Attribution 4.0 International License (<http://creativecommons.org/licenses/by/4.0/>), which permits unrestricted use, distribution, and reproduction in any medium, provided you give appropriate credit to the original author(s) and the source, provide a link to the Creative Commons license, and indicate if changes were made.

References

- Ramalingam B, Khan MMR, Mondal B, Mandal AB, Das SK (2015) Facile synthesis of silver nanoparticles decorated magnetic-chitosan microsphere for efficient removal of dyes and microbial contaminants. *ACS Sustain Chem Eng* 3:2291–2302
- Vîrlan C, Ciocârlan RG, Roman T, Gherca D, Cornei N, Pui A (2013) Studies on adsorption capacity of cationic dyes on several magnetic nanoparticles. *Acta Chem IAS* 21:19–30
- Fisli A, Yusuf S, Ridwan YK, Krisnandi JG (2014) Preparation and characterization of magnetite-silica nano-composite as adsorbents for removal of methylene blue dyes from environmental water samples. *Adv Mater Res* 896:525–531
- Jiang Z, Xie J, Jiang D, Yan Z, Jing J, Liu D (2014) Enhanced adsorption of hydroxyl contained/anionic dyes on nonfunctionalized Ni@SiO₂core-shell nanoparticles: kinetic and thermodynamic profile. *Appl Surf Sci* 292:301–310
- Haldorai Y, Shim J-J (2014) An efficient removal of methyl orange dye from aqueous solution by adsorption onto chitosan/



- MgO composite: a novel reusable adsorbent. *Appl Surf Sci* 292:447–453
6. Tang L, Cai Y, Yang G, Liu Y, Zeng G, Zhou Y, Li S, Wang J, Zhang S, Fang Y, He Y (2014) Cobalt nanoparticles-embedded magnetic ordered mesoporous carbon for highly effective adsorption of rhodamine B. *Appl Surf Sci* 314:746–753
 7. Amaranatha Reddy D, Lee S, Choi J, Park S, Ma R, Yang H, Kim TK (2015) Green synthesis of AgI-reduced graphene oxide nanocomposites: toward enhanced visible-light photocatalytic activity for organic dye removal. *Appl Surf Sci* 341:175–184
 8. Wang J, Tsuzuki T, Bin Tang A, Sun XJ, Dai GD, Rajmohan JL, Wang X (2014) Recyclable textiles functionalized with reduced graphene oxide@ZnO for removal of oil spills and dye pollutants. *Aust J Chem* 67:71–77
 9. Kong LP, Gan XJ, bin Ahmad AL, Hamed BH, Evarts ER, Ooi BS, Lim JK (2012) Design and synthesis of magnetic nanoparticles augmented microcapsule with catalytic and magnetic bifunctionalities for dye removal. *Chem Eng J* 197:350–358
 10. Deng J-H, Zhang X-R, Zeng G-M, Gong J-L, Niu Qiu-Ya, Liang J (2013) Simultaneous removal of Cd(II) and ionic dyes from aqueous solution using magnetic graphene oxide nanocomposite as an adsorbent. *Chem Eng J* 226:189–200
 11. Zhang Y-R, Shen S-L, Wang S-Q, Huang J, Peng S, Wang Q-R, Zhao B-X (2014) A dual function magnetic nanomaterial modified with lysine for removal of organic dyes from water solution. *Chem Eng J* 239:250–256
 12. Fegade U, Singh A, Krishna Chaitanya G, Singh N, Attarde S, Kuwar A (2014) Highly selective and sensitive receptor for Fe³⁺ probing. *Spectrochim Acta Part A Mole Biomole Spectr* 121:569–574
 13. Fegade U, Tayade S, Krishna Chaitanya G, Attarde S, Kuwar A (2014) Fluorescent and chromogenic receptor bearing amine and hydroxyl functionality for iron(III) detection in aqueous solution. *J Fluoresc* 24:675–681
 14. Fegade U, Saini A, Sahoo SK, Singh N, Bendre R, Kuwar A (2014) 2,2'-(Hydrazine-1,2-diylidenedimethylidene) bis(6-isopropyl-3-methylphenol) based selective dual-channel chemosensor for Cu²⁺ in semiaqueous media. *RSC Adv* 4:39639–39644
 15. Fegade U, Sahoo SK, Attarde S, Singh N, Kuwar A (2014) Colorimetric and fluorescent “On-Off” chemosensor for Cu²⁺ in semiaqueous medium. *Sens Actuators B* 202:924–928
 16. Fegade U, Sharma H, Attarde S, Singh N, Kuwar A (2014) Urea based dipodal fluorescence receptor for sensing of Fe³⁺ ion in semi-aqueous medium. *J Fluoresc* 24:27–37
 17. Fegade U, Sharma H, Bondhopadhyay B, Basu A, Attarde S, Singh N, Kuwar A (2014) Turn-on” fluorescent dipodal chemosensor for nano-molar detection of Zn²⁺: application in living cells imaging. *Talanta* 125:418–424
 18. Kuwar A, Fegade U, Tayade K, Patil U, Puschmann H, Gite V, Dalal D, Bendre RS (2013) Bis(2-hydroxy-3-isopropyl-6-methylbenzaldehyde) ethylenediamine: a novel cationsensor. *J Fluoresc* 23:859–864
 19. Fegade U, Attarde S, Sahoo SK, Singh N, Kuwar A (2014) A selective and discriminating noncyclic receptor for HSO₄⁻ ion recognition: 2, 2-(pyridine-2,6-diylbis(azanediyl)) bis (methylene) diphenol. *RSC Adv* 4:15288–15292
 20. Fegade U, Sahoo SK, Singh A, Singh N, Attarde S, Kuwar A (2015) *Anal Chim Acta* 872:63–69
 21. Jethave G, Fegade U, Attarde S, Ingle S (2017) Facile synthesis of lead doped zinc-aluminum oxide nanoparticles (LD-ZAO-NPs) for efficient adsorption of anionic dye: kinetic, isotherm and thermodynamic behaviors. *J Indus Eng Chem* 53:294–306
 22. Fegade U, Jethave G, Su K-Y, Huang W-R, Wu R-J (2018) An multifunction Zn_{0.3}Mn_{0.4}O₄ nanospheres for carbon dioxide reduction to methane via photocatalysis and reused after fifth cycles for phosphate adsorption. *J Environ Chem Eng*. <https://doi.org/10.1016/j.jece.2018.02.040>
 23. Crini G (2008) Kinetic and equilibrium studies on the removal of cationic dyes from aqueous solution by adsorption onto a cyclodextrin polymer. *Dyes Pigments* 415–426
 24. Langmuir L (1918) The adsorption of gases on plane surfaces of glass, mica and platinum. *J Am Chem Soc* 40:1361–1403
 25. Freundlich H, Heller W (1939) The adsorption of cis- and trans-azobenzene. *J Am Chem Soc* 61:2228–2230
 26. Temkin MJ, Pyzhev V (1940) *Acta Physiochim USSR* 12:217–222
 27. Weber TW, Chakravorti RK (1974) Pore and solid diffusion models for fixed-bed adsorbers. *J Am Inst Chem Eng* 209:228–238
 28. Stumm W, Morgan JJ (1995) *Aquatic chemistry: chemical equilibrium and rates in natural waters*, 3rd edn. Wiley, New York, p 1040
 29. Liu R, Hongxia F, Yin H, Lu PL, Tao Y (2015) A facile sol combustion and calcination process for the preparation of magnetic Ni_{0.5}Zn_{0.5}Fe₂O₄ nanopowders and their adsorption behaviors of Congo red. *Powder Tech* 274:418–425
 30. Girgis E, Adel D, Tharwat C, Attallah O, Rao KV (2015) Cobalt ferrite nanotubes and porous nanorods for dye removal. *Adv Nano Res* 3:111–121
 31. Yang S, Zhaohui W, Huang L, Zhou B, Lei M, Sun L, Tian Q, Pan J, Wei W, Zhang H (2014) Significantly enhanced dye removal performance of hollow tin oxide nanoparticles via carbon coating in dark environment and study of its mechanism. *Nanoscale Res Lett* 442:1–9
 32. Liu R, Tian Y, Jintao X, Hongxia F, Li Y (2016) Efficient removal of Congo Red by magnetic CoFe₂O₄ nanoparticles prepared via the rapid combustion process. *J Nanosci Nanotechnol* 16:9535–9543
 33. Liu R, Hongxia F, Yimin L, Yin H, Lequn Yu, Ma L, Han J (2016) Adsorption optimization and mechanism of neutral red onto magnetic Ni_{0.5}Zn_{0.5}Fe₂O₄/SiO₂ nanocomposites. *J Nanosci Nanotechnol* 16:8252–8262
 34. Liu R, Lv P, Hongxia F, Rongzhu L, Xiaoyang W, Yimin L (2017) Removal performance of methyl blue onto magnetic MgFe₂O₄ nanoparticles prepared via the rapid combustion process. *J Nanosci Nanotechnol* 17:4755–4762
 35. Zheng Y, Zhu B, Chen H, You W, Jiang C, Jiaguo Yu (2017) Hierarchical flower-like nickel(II) oxide microspheres with high adsorption capacity of Congo red in water. *J Colloid Interface Sci* 504:688–696
 36. Lei C, Zhu X, Zhu B, Yu J, Ho W (2016) Hierarchical NiO–SiO₂ composite hollow microspheres with enhanced adsorption affinity towards Congo red in water. *J Colloid Interface Sci*. 466:238–246
 37. Zhichao Yu, Liu B, Zhou H, Feng C, Wang X, Yuan K, Gan X, Zhu L, Zhang G, Dong X (2017) Mesoporous ZrO₂ fibers with enhanced surface area and the application as recyclable adsorbent. *Appl Surf Sci* 399:288–297
 38. Xiaofei W, Wang W, Li F, Khaimanov S, Tsidaeva N, Lahoubi M (2016) PEG-assisted hydrothermal synthesis of CoFe₂O₄ nanoparticles with enhanced selective adsorption properties for different dyes. *Appl Surf Sci* 389:1003–1011
 39. Lei C, Pi M, Jiang C, Cheng B, Jiaguo Yu (2017) Synthesis of hierarchical porous zinc oxide (ZnO) microspheres with highly efficient adsorption of Congo red. *J Colloid Interface Sci* 490:242–251
 40. Aliabadi RS, Mahmoodi NO (2018) Synthesis and characterization of polypyrrole, polyaniline nanoparticles and their nanocomposite for removal of azo dyes; sunset yellow and Congo red. *J Cleaner Prod* 179:235–245
 41. Ealias AM, Saravanakumar MP (2018) Facile synthesis and characterisation of AlNs using protein rich solution extracted from sewage sludge and its application for ultrasonic assisted dye



- adsorption: isotherms, kinetics, mechanism and RSM design. *J Environ Manag* 206:215–227
42. Xu J, Xu D, Zhu B, Cheng B, Jiang C (2018) Adsorptive removal of an anionic dye Congo red by flower-like hierarchical magnesium oxide (MgO)-graphene oxide composite microspheres. *Appl Surf Sci* 435:1136–1142

Publisher's Note Springer Nature remains neutral with regard to jurisdictional claims in published maps and institutional affiliations.